BBA Advances 2 (2022) 100033

Contents lists available at ScienceDirect

BBA Advances

journal homepage: www.sciencedirect.com/journal/bba-advances

Ab initio reconstruction of small angle scattering data for membrane proteins in copolymer nanodiscs

Kerrie A. Morrison [a,b,c], Aswin Doekhie [a], George M. Neville [a,c], Gareth J. Price [a,d], Paul Whitley [b], James Doutch [e,*], Karen J. Edler [a,*]

[a] Department of Chemistry, University of Bath, Bath, UK
[b] Department of Biology and Biochemistry, University of Bath, Bath, UK
[c] Centre for Sustainable and Circular Technologies, University of Bath, Bath, UK
[d] Department of Chemistry, Khalifa University, Abu Dhabi, UAE
[e] ISIS Pulsed Neutron and Muon Source, Rutherford Appleton Laboratory, Harwell Oxford, Didcot OX11 0QX. UK

ARTICLE INFO

Keywords:
Nanodisc
SMALP
Ab initio
Small angle neutron scattering
Outer membrane protein F
MONSA

ABSTRACT

Background: Small angle scattering techniques are beginning to be more widely utilised for structural analysis of biological systems. However, applying these techniques to study membrane proteins still remains problematic, due to sample preparation requirements and analysis of the resulting data. The development of styrene-maleic acid co-polymers (SMA) to extract membrane proteins into nanodiscs for further study provides a suitable environment for structural analysis.

Methods: We use small angle neutron scattering (SANS) with three different contrasts to determine structural information for two different polymer nanodisc-incorporated proteins, Outer membrane protein F (OmpF) and gramicidin. *Ab initio* modelling was applied to generate protein/lipid structures from the SANS data. Other complementary structural methodologies, such as DLS, CD and TEM were compared alongside this data with known protein crystal structures.

Results: A single-phase model was constructed for gramicidin-containing nanodiscs, which showed dimer formation in the centre of the nanodisc. For OmpF-nanodiscs we were able to construct a multi-phase model, providing structural information on the protein/lipid and polymer components of the sample.

Conclusions: Polymer-nanodiscs can provide a suitable platform to investigate certain membrane proteins using SANS, alongside other structural methodologies. However, differences between the published crystal structure and OmpF-nanodiscs were observed, suggesting the nanodisc structure could be altering the folding of the protein.

General significance: Small angle scattering techniques can provide structural information on the protein and polymer nanodisc without requiring crystallisation of the protein. Additional complementary techniques, such as *ab initio* modelling, can generate alternative models both the protein and nanodisc system.

1. Introduction

The difficulties in the extraction and study of membrane proteins have been widely documented [1–3]. Their roles within living organisms are extensive and include cell-to-cell communication, recognition, and movement. Additionally, membrane proteins control which molecules may enter or leave through membranes; allowing molecules needed for energy, cell growth and repair to enter whilst expelling harmful substances. Membrane proteins account for around 20-30 % of the proteome within many organisms [4,5,6]. However, unlike their soluble protein counterparts, structural and functional knowledge of membrane proteins is severely lacking. Due to their location within a lipid membrane, making them amphipathic in nature, these proteins are often sensitive to environmental changes and are liable to misfolding

Abbreviations: CD, circular dichroism; DLS, dynamic light scattering; DMPC, 1,2-dimyristoyl-sn-glycero-3- phosphocholine; MP, membrane protein; OmpF, Outer membrane protein F; SANS, small angle neutron scattering; SAS, small angle scattering; SAXS, small angle X-ray scattering; SEC, size exclusion chromatography; SMA, styrene-maleic acid copolymer; SMALP, styrene-maleic acid lipid particles; TEM, transmission electron microscopy.

* Corresponding authors.
E-mail addresses: james.doutch@stfc.ac.uk (J. Doutch), k.edler@bath.ac.uk (K.J. Edler).

https://doi.org/10.1016/j.bbadva.2021.100033

Available online 16 December 2021

when removed from their natural lipid bilayer environment. Both structural and functional studies frequently require purified membrane protein samples. The most widely used method of extracting membrane proteins for purification is through the use of detergents. These form micelles, or in uncommon cases, bicelles, which can be used to extract membrane proteins from their lipid bilayer environment to be studied. This process typically removes annular lipids surrounding the membrane protein, which opens up the possibility of protein degradation and mis-folding, as these environments are unstable compared to their native bilayer. These difficulties have caused a bottleneck in membrane protein study, with less than 1% of all three-dimensional protein structures in the Protein Data Bank (PDB) accounting for integral membrane proteins [7–9], highlighting the void of information in this regard.

Other methods for protein extraction have also been developed, such as amphipols or creating nanodiscs using membrane-scaffold proteins (MSPs), a genetically engineered protein based on the human protein apolipoprotein A-1 [10]. However, these methods can be expensive and often involve time-consuming optimisation or design. Additionally, MSPs require detergents for the initial extraction of the membrane protein, before incorporation into the more stable nanodisc environment, thus retaining the chance for protein mis-folding caused by detergent extraction. A recent development within this field is the use of styrene-maleic acid co-polymers (SMA) [11] and other copolymers, such as diisobutylene maleic acid (DIBMA) [12], which can extract nanodiscs directly from the membrane, without the prior use of detergents [11, 13], making a more stable, detergent-free environment for membrane proteins to be studied. It is hoped that the bilayer nanodisc can create a "native-like" environment to study these elusive proteins more thoroughly.

Once extracted, there are a wide variety of methods available to study structural interactions, or dynamic information for proteins and bio-macromolecules. Some of the more common techniques include cryo-electron microscopy (cryo-EM), and nuclear magnetic resonance spectroscopy (NMR), which recently have improved resolution and continue to develop and build more powerful instruments [14,15]. However, X-ray crystallography is still the most widely-used method for obtaining three-dimensional structural information for proteins at an atomic level [16]. The study of protein structure and function has utilised a wide variety of analytical methods, and techniques such as small angle scattering (SAS) can provide an another, complementary avenue to investigate complex biomolecule systems [14,17–19]. Unlike cryo-EM or X-ray crystallography, which require frozen samples or well-diffracting crystals respectively, SAS experiments are usually conducted on aqueous solutions [14,20].

Small angle scattering (SAS) is a useful tool for determining structural information in several different areas. Small angle neutron scattering (SANS) is useful for gathering structural data, and in many ways is complementary to other structural analysis techniques, such as dynamic light scattering (DLS), circular dichroism (CD) and small angle X-ray scattering (SAXS). One of the principal advantages of SANS is the ability to utilise selectively deuterated components in combination with hydrogenated materials to "mask out" parts of a system, by using contrast variation/matching. For protein scattering this is usually achieved by adjusting the D_2O/H_2O ratio within the buffer solution due to the difficulties inherent in deuterating the native lipids or the protein itself. Such methods are especially useful when characterising multi-component systems, such as polymer-nanodiscs, which have polymer, lipid, solvent, and protein elements within a sample. Nanodisc samples are well suited for neutron scattering experiments, as they are stable under long data acquisition, and can be synthesised in sufficient quantity and concentration, whilst maintaining low polydispersity.

From previous SANS studies, a nanodisc model was generated with which to fit and analyse the data using software developed at NIST [21]. This model was found suitable to fit lipid-only nanodiscs without the protein incorporated. However, the insertion of membrane protein into the nanodisc adds further complexity, requiring changes to model parameters to accommodate such structures. Fig. 1 shows the overall shape for the circular cylindrical model and the typical parameters (Table 1) we have previously found when examining lipid-only nanodiscs, containing 1,2-dimyristoyl-sn-glycero-3-phosphocholine (DMPC). In this model the central cylinder represents a circular patch of DMPC bilayer, with headgroup slabs at either end of the core which is composed of the lipid tails. The polymer forms a circular belt around the lipid tail region of the cylinder, to shield the hydrophobic tails from the surrounding aqueous solution, but does not overlap with the headgroup regions.

One of the difficulties thus far in determining the shape of the nanodiscs using SAS, is the use of a deterministic form factor model, with the overall particle shape assumed to be, for example nanodiscs or a core-shell sphere. Specifically, these models assume that the fitted shapes or form factors, i.e. spheres, ellipses or cylinders are uniform and form distinct layers within the structure. It is possible in principle to correct shape effects by using larger polydispersity terms to effectively 'blur' the structure. However, this is clearly of limited utility when attempting to obtain accurate structural dimensions. One complementary technique to determine structures from SAS data is *ab initio*

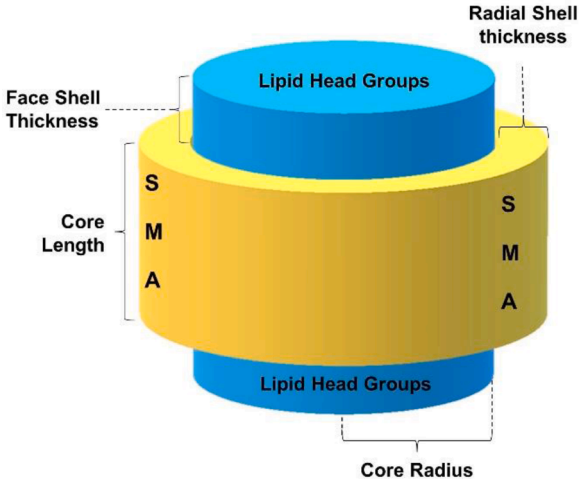

Fig. 1. Schematic of nanodisc model used to fit SANS data. Model adapted from [24].

Table 1
Parameters and typical values for the nanodisc model used to fit SANS data from nanodiscs prepared using the copolymer SMA2000. The values of the following parameters: core length, face shell thickness, SLD core, mole fraction of water in face (Mol frac. H_2O in face), SLD solvent, concentration of monovalent salt in sample solution (Conc. Monovalent Salt), dielectric constant and temperature were fixed. [Mol frac. in belt] corresponds to the mole fraction of water in the polymer belt. (*) denote the parameters allowed to fit the data. Parameters are described in Jamshad et.al., [23].

Parameters	Units	Values
Volume Fraction		0.04*
Mean Core Radius	Å	40*
Polydispersity		0.35*
Core Length	Å	28
Radial Shell Thickness	Å	10*
Face Shell Thickness	Å	8
SLD core	$Å^{-2}$	5×10^{-7}
Mol frac. H_2O in face		0.57
Mol frac. H_2O in belt		0.6*
SLD solvent	$Å^{-2}$	6×10^{-6}
Charge		40
Conc. Monovalent Salt	mol/L	0.1665
Dielectric constant		78
Temperature	K	298
Background		0.01*

modelling. *Ab initio* modelling creates possible conformational structures based on simulated annealing of the input data, rather than using pre-determined structures. This methodology is frequently applied to soluble proteins of various molecular weights and is used to obtain solution structures of proteins and their complexes at low resolution. DAMMIN is a single-phase ab initio modelling tool, where a phase represents either a protein or the solvent. This creates models that are made up of beads termed by the authors as "dummy atoms", which are assigned to represent protein or solvent. MONSA is an extension of this methodology, which is able to derive models with multiple phases simultaneously, based on differences in scattering length density (SLD). MONSA was specifically optimised for modelling with SANS data, as it can draw upon multiple datasets to highlight the different aspects of the system to obtain a clearer understanding of the whole structure, by assigning the "dummy atoms" to different phases within the system or solvent. This methodology and software was developed by Svergun et al., [22] and can be used to determine low-resolution dummy-atom models, by inputting the correct scattering length densities to each of the datasets; i.e. the polymer belt, and the combined lipid/protein core.

In this study we utilise SMA as a support for two membrane proteins: Outer membrane protein F (OmpF) and gramicidin. Gramicidins are a form of ionophore, which can form channels to allow cations across mitochondrial membranes and other lipid bilayers [25–27]. Gramicidin A is also a well-known antibiotic, which is able to disrupt cellular ionic homeostasis [28]. As gramicidin is able to permeate to form integral peptides across the lipid bilayer and is readily available in large quantities commercially, it was considered a suitable protein to test our methodology. Additionally, by using simple lipids, such as DMPC, known to form nanodiscs in the presence of SMA [29], this would eliminate the complexity of using natural biological membranes. OmpF is a membrane protein found on the outer membrane of gram-negative bacteria, such as Escherichia coli (E. coli). This protein facilitates the transport of small hydrophilic molecules, less than 600 Daltons, across the outer membrane [30, 31]. OmpF is a 16 β-stranded barrel and is one of two membrane porins which make up approximately 7 % of the total protein within a cell, equating to 10^5 copies per cell on average [32,33]. OmpF can form a homotrimer, consisting of 37 kDa monomer units [33, 34]. OmpF was one of the earliest membrane protein porin structures to be determined [33–36]. The extensive characterisation of this system renders it an ideal candidate for testing new methodology, in order to determine the potential pitfalls or differences associated with modelling membrane protein structures, ab initio, from SANS data using polymer-derived nanodiscs.

In this work, the structure of OmpF and gramicidin has been investigated within nanodiscs using form-factor based SANS fitting methods for comparison to dummy-atom models generated using the *ab initio* modelling tools, DAMMIN and MONSA. This paper highlights the structures of OmpF, and gramicidin proteins incorporated in polymer-nanodiscs determined using SANS, how they compare to other techniques, such as DLS and CD, and discusses differences that occur when modelling these complex systems using different methods, whilst comparing to known protein crystal structures.

2. Materials and methods

2.1. Materials

1,2-dimyristoyl-sn-glycero-3-phosphocholine (hDMPC) and deuterated 1,2-dimyristoyl-d54-sn-glycero-3-phosphocholine (d-DMPC) were purchased from Avanti Polar Lipids Ltd. The poly(styrene-co-maleic anhydride), SMA® 2000 was purchased from Cray Valley. Slide-A-Lyser® Mini dialysis units at 10,000 MWCO (#11809420), Vivaspin 500 centrifugal concentrators at 3000 MWCO (#10440282) were purchased from Fisher Scientific. Disposable PD 10 Desalting Columns (Cytiva, #17-0851-01PD-10), Gramicidin from Bacillus aneurinolyticus (Bacillus brevis) (#G5002) and all other chemicals were purchased from Sigma Aldrich and used without further purification.

2.2. Polymer hydrolysis

The commercially available SMA2000 is a poly(styrene-co-maleic anhydride) copolymer (SMAnh), insoluble in water and supplied by Cray Valley (SMA® 2000). It was hydrolysed to its acid form – poly (styrene-co-maleic acid), (SMA). Hydrolysis was conducted as with previous work [37,38]. In summary, a solution of 10% w/v SMAnh in 2 mol dm^{-3} NaOH was heated under reflux for 2 h. The solution was cooled and the product precipitated by reducing the pH to below 3.0 using concentrated hydrochloric acid. The polymer was recovered by centrifugation at 10,000 x g and washed three times with deionised water, before re-dissolving in 2 mol dm^{-3} NaOH and adjusting to pH 8.0. The final solution was then freeze-dried.

2.3. Gramicidin SANS sample preparation

To prepare gramicidin-nanodiscs, a mixture of gramicidin-DMPC liposomes was prepared at a stock concentration of 20 mM DMPC with 320 μM gramicidin. First, a mixture of DMPC and gramicidin was prepared in a solution of 1:1 chloroform: methanol. The solution was then dried using a rotary evaporator to create a thin film. The film was then rehydrated with PBS buffer (35 mM sSodium phosphate dibasic, 150 mM NaCl) prepared in H_2O (h-PBS), D_2O (d-PBS) or 32 mol% D_2O in H_2O (32% d-PBS) to create gramicidin-incorporated vesicles. SMA was added to a final concentration of 10 mM DMPC, 160 μM gramicidin and 2.5% (w/v) SMA. This was repeated for each deuteration contrast used for SANS; d-DMPC with h-PBS, h-DMPC with d-PBS and d-DMPC with 32% d-PBS.

2.4. OmpF enrichment

Endogenous OmpF enrichment was adapted from Efremov and Sazanov [39]. In summary, E.coli cells were resuspended, homogenised and broken in a French Press or continuous flow disruptor. The sample was centrifuged at 9,700 x g for 15 minutes and the cell lysate (supernatant) was collected. The membranes were pelleted through centrifugation at 23,800 x g for 30 to 90 min. Membrane fractions E.coli cells, were re-suspended in 25 mL PB buffer (20 mM Tris pH 8.0, 1 mM EDTA). 1 % (w/v) Triton X-100 was added to the membrane samples and left for 15 minutes with gentle agitation to solubilise inner membranes. Samples were then ultra-centrifuged at 178,000 x g for 40 min at 4 °C to remove inner membrane and Triton X-100 contaminants which remain in the supernatant. The pellet was then harvested, re-suspended in PB buffer and homogenised. Next, 2% (w/v) Triton X-100 was added to the sample and left to stir for 10 minutes at room temperature. OmpF enriched membrane pellets were collected through ultra-centrifugation at 178, 000 x g, for 40 min at 4°C to remove any remaining species solubilised by the Triton X-100 which again remain in the supernatant. The pellets were solubilised with SMA2000 at a final concentration of 2.5 (w/v). Samples were incubated for 1 h with gentle agitation at room temperature, before ultra-centrifugation at 120,000 x g for 20 min at 4 °C. The supernatant was collected, and excess polymer removed from the sample using size exclusion chromatography (SEC). A Superdex^{TM} 200 10/300 column (GE Healthcare) was used to separate the solubilised nanodiscs from the excess polymer within the sample using an AKTA FPLC purification system. Fractions containing nanodiscs were collected and underwent lipid exchange for SANS experimentation. A DLS measurement was made on the fractionated nanodiscs containing the native lipid.

2.5. Circular dichroism

Circular dichroism (CD) spectra were measured between 260 – 185 nm at 20°C using a 1.00 mm quartz cuvette using a Chirascan CD spectrometer (Applied Photophysics, UK) to confirm that the protein

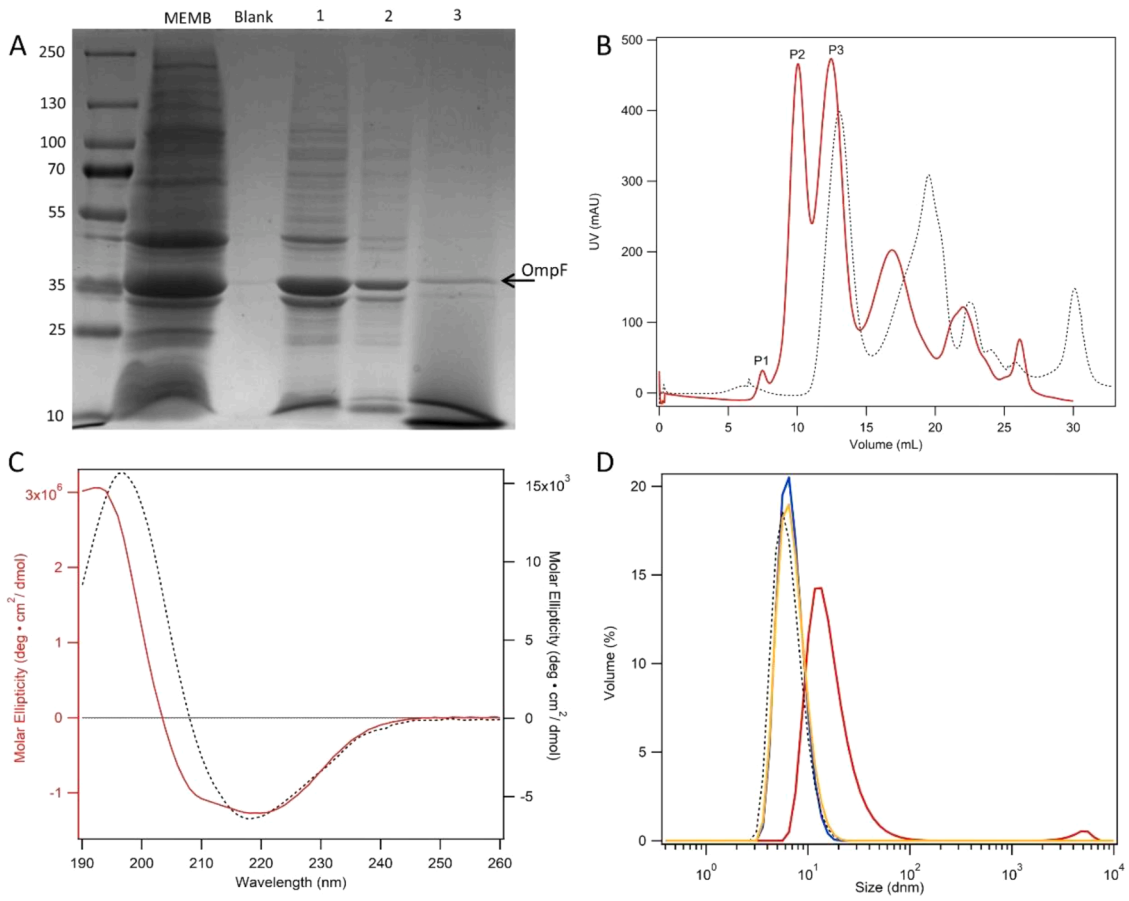

Fig. 2. [A] Coomassie stain of the OmpF purification process (MEMB) depicts the crude membrane sample prior to purification, (1 and 2) show the pelleted sample harvested from the initial and second Triton solubilisation centrifugation steps; (3) shows the purified sample using 2.5 % (w/v) SMA2000; black arrow highlights OmpF band [B] SEC chromatogram from OmpF nanodisc sample (red) and DMPC-lipid nanodisc sample (black, dashed) at 254nm wavelength. [C] CD spectra for OmpF incorporated in nanodiscs (peak 3, red), ranging from 260 – 190 nm compared to a predicted CD spectra for OmpF crystal structure (PDB ID: 2OMF, black dotted), determined by PDBMD2CD [50]; [D] DLS data comparing the overall diameters of nanodiscs incorporating OmpF prior to (red) and after lipid-exchange (yellow), nanodiscs incorporating gramicidin (blue) and empty DMPC nanodiscs (dotted black).

was incorporated into the nanodiscs. The OmpF-enriched nanodisc sample from Peak 3 was dialysed into sodium phosphate buffer at pH 7.8 using a disposable PD-10 desalting column. The preparation of OmpF samples for CD requires a buffer exchange to reduce solvent interference. A disposable PD 10 Desalting Column was used to exchange the PB buffer to sodium phosphate buffer (pH 7.8), following the manufacturers protocol. UV absorbance was read to determine the protein concentration, before diluting to 0.2 mg/mL for CD analysis. DMPC-only nanodiscs were used as a control. To remove any 'background' interference from the CD spectrum, the signal from the DMPC-only nanodisc sample was subtracted from that from the OmpF samples. Scans were recorded with a bandwidth of 2 nm, 1 nm step increments, a 2 s time-per-point, and repeated 5 times. Scans were then averaged and normalised from millidegrees (instrument units) to delta epsilon ($\Delta\varepsilon$) in M^{-1} cm^{-1}. The data was analysed using Dichroweb [40–42] to determine the nature of the protein structure within the nanodiscs.

2.6. Lipid exchange

In order to obtain samples with deuterated lipid contrasts to study using SANS, purified OmpF samples in nanodiscs, initially containing native lipids, were subjected to lipid exchange. First, samples of 10 mM deuterated-DMPC (d-DMPC) with 1.5% (w/v) SMA in PBS buffer (20 mM Tris pH 8, 150 mM NaCl), were left for 1 h at room temperature under gentle agitation. Excess polymer was removed by SEC using a Superdex^{TM} 200 10/300 column. Fractions were collected and lipid samples were concentrated by ultrafiltration using 3000 MWCO Ultra Centrifugal Filters to 10 mM d-DMPC, before adding to OmpF nanodisc samples at a 2:1 ratio of OmpF nanodiscs to d-DMPC nanodiscs. Samples were left overnight at 4 °C with gentle agitation to ensure lipid exchange had occurred. DLS was measured on the lipid exchanged nanodiscs after this step. This sample was split into three equal parts, ready for buffer exchange.

In order to obtain the final buffer contrasts for SANS experimentation, buffer exchange was required through dialysis. Samples required a 100% deuterated PBS (d-PBS; made using D_2O) and 32% d-PBS contrast (prepared using 32 mol % D_2O and 68 mol % H_2O in the PBS) to mask out hydrogenated polymer. This was done using 10,000 MWCO mini dialysis units and left overnight with at least 2 buffer changes to ensure sufficient exchange. Examples of the final samples were as follows; polymer with hydrogenated-natural bacterial membrane (h-bact) in 100% deuterated PBS (d-PBS); polymer with partially deuterated bacterial membranes via. lipid exchange with d-DMPC (d-bact) in 100% d-PBS; polymer with d-bact membranes in hydrogenated-PBS (h-PBS); and lastly polymer with d-bact membranes in 32 % d-PBS.

2.7. SANS

Nanodisc solutions were loaded into 1mm thick quartz Hellma cells and placed in a temperature-controlled sample holding rack at 25 °C. Measurements were made on the SANS2d instrument at ISIS Neutron and Muon source (Harwell, UK). A source to sample and sample to

Table 2
Table showing the deconvolution values obtained from Dichroweb [40–42] for nanodiscs incorporating OmpF (OmpF-SMA), normalized root-mean-square deviation (NRMSD) = 0.018. Values are compared to the crystal structure for OmpF (PDB ID: 2OMF) using STRIDE [51] and 2StrucCompare web interface to calculate the secondary structures. [Helix 1 and Helix 2] correspond to the α-helices, [Strand 1 and Stand 2] correspond to the β-sheets, [Turns] correspond to the turns in the protein structure and [unordered] equate to disordered sections within the protein.

	Helix1	Helix2	Strand1	Strand2	Turns	Unordered	Total
OmpF-SMA	0.03	0.05	0.23	0.12	0.22	0.33	0.98
	0.08		0.35		0.55		0.98
2OMF STRIDE	0.04		0.58		0.38		1.00

detector distance of 4 m was used, with 8 mm beam size at the sample position, giving q range 0.004 $Å^{-1}$ to 0.7 $Å^{-1}$. The scattering from a polymer standard was used to normalise the data onto an absolute scale. Data were corrected, solvent backgrounds subtracted and reduced to 1-D curves using Mantid software [43]. A circular cylindrical nanodisc model [21] was used for the gramicidin-nanodiscs, whereas an ellipsoidal cylindrical nanodisc model was used to fit OmpF-nanodiscs [44]. In this case, the ellipticity of the core cross section was described by two radii; the major and minor radius, which are linked by the ellipticity. The model is part of the SANS analysis software developed at NIST [21], modified to incorporate the water content in the shell. SANS data at different contrasts were globally/simultaneously fitted to determine the overall parameters of the nanodisc, using the NIST SANS analysis package within Igor Pro 6 (Wavemetrics) software [21].

2.8. Dynamic light scattering

DLS measurements were taken for DMPC lipid only nanodiscs and gramicidin-nanodiscs. Measurements on two OmpF-nanodiscs samples were also taken, both prior to, and after lipid exchange. All DLS measurements were performed using a Malvern Panalytical Zetasizer Nano ZS at 25 °C, in disposable 40 μl micro cuvettes, at a wavelength of 633 nm and an angle of 173°. Size distribution was measured using the Zetasizer software and is shown on a log scale, plotted using Igor Pro 6 (Wavemetrics) software.

2.9. Transmission electron microscopy

For transmission electron microscopy (TEM), imaging samples were prepared as follows; carbon-formvar coated copper grids were activated by glow discharge before applying 10 μL sample (diluted to 20 μg/mL) for 1 min. The grid was then blotted before washing with DI water and blotted again. The grid was then stained with uranyl acetate before allowing to dry. The images were taken using a Jeol 2100 TEM instrument at 200 kV.

2.10. Gramicidin nanodisc SANS data ab initio modelling

DAMMIF was used to create an overall shape before further refinement. DAMMIF models were repeated ten times with no symmetry (P1), before being passed through a series of model evaluations; First, DAMSEL, which transposes each repeat to highlight potential outliers within the models. This was followed by DAMSUP, which can transpose the repeats and assigns a probability weighting for each dummy atom. Next, DAMAVER [45] was used to average the models and align to the same axis. DAMFILT was then used to remove any artifacts within the models. These models were then converted via DAMSTART to be passed through DAMMIN [22], to compare against the original data file. DAMMIN is the slower mode software for single phase shape determination, to obtain the most accurate "dummy atom" model for the data inputted [46].

2.11. OmpF nanodisc SANS data ab initio modelling

MONSA was used to generate a multi-phase model of two phases for the OmpF-nanodisc system. Further refinement of these models was as follows; The MONSA models for each of the two phases were first run through DAMSEL, to transpose each repeat into the same orientation and to highlight potential outlier "dummy atoms"; next through DAMSUP, to determine probability weightings for each "dummy atom"; followed by DAMAVER, which averages the models and aligns them to the same axis' and lastly though DAMSTART and DAMFILT separately, removing artifacts [45,47]. The resulting two models were superimposed at the correct orientation to one another by using SUPCOMB [48] and visualised using Visual Molecular Dynamics (VMD) [49] software.

3. Results and discussion

3.1. OmpF enrichment

The solubilisation of OmpF with SMA has not been previously reported, therefore the first step was to determine whether this could be achieved. The results in Fig. 2A, show the enrichment process starting from crude membrane (MEMB), through purification with Triton X-100 (lanes 1 and 2), and lastly the OmpF enriched fraction was incorporated into polymer nanodiscs using SMA (lane 3). Although there is a loss of protein along each step, the high quantity of OmpF present within samples results in highly enriched samples at a concentration suitable for further characterisation (approximately 1 mg/mL). It should be noted that the outer membranes containing OmpF are prepared for SMA solubilisation following detergent solubilisation of inner membrane. Therefore, the incorporation of OmpF into polymer nanodiscs is not a detergent-free procedure.

3.2. SEC sample peaks

To reduce the polydispersity of the sample for SANS measurements, OmpF nanodisc samples were fractionated from aggregates and free, unbound polymer using SEC with detection at 254nm to highlight the polymer. The first peak (seen in Fig. 2B, P1) was calculated to be at the void volume (V_O) (Standards can be found in appendix, Fig. A.1), suggesting large polymer aggregates within the sample. Peak 2 (P2) was calculated to be at approximately 154 kDa and peak 3 (P3) at approximately 85 kDa. It was thought the OmpF nanodiscs would either be in P2 or P3, as OmpF in trimer form is around 110 kDa and in monomer form approximately 37 kDa [33,34]. In comparison, lipid-only nanodiscs had a peak of approximately 67 kDa, smaller than P3 (Fig. 2B). The remaining peaks are commonly seen in SEC data from solutions of SMA2000 and are thought to be free polymer.

3.3. Circular dichroism of OmpF samples

The spectrum from the protein-containing nanodisc was compared to a known OmpF protein structure (PDB ID: 2OMF) (Fig. 2.C). The predicted CD spectrum for OmpF structure 2OMF, was determined by PDBMD2CD [50]. Values for the crystal structure were obtained through the 2StrucCompare web interface using the STRuctural IDEntification method (STRIDE)[51] to determine the secondary structures in the sample. These can be compared to the values calculated for the

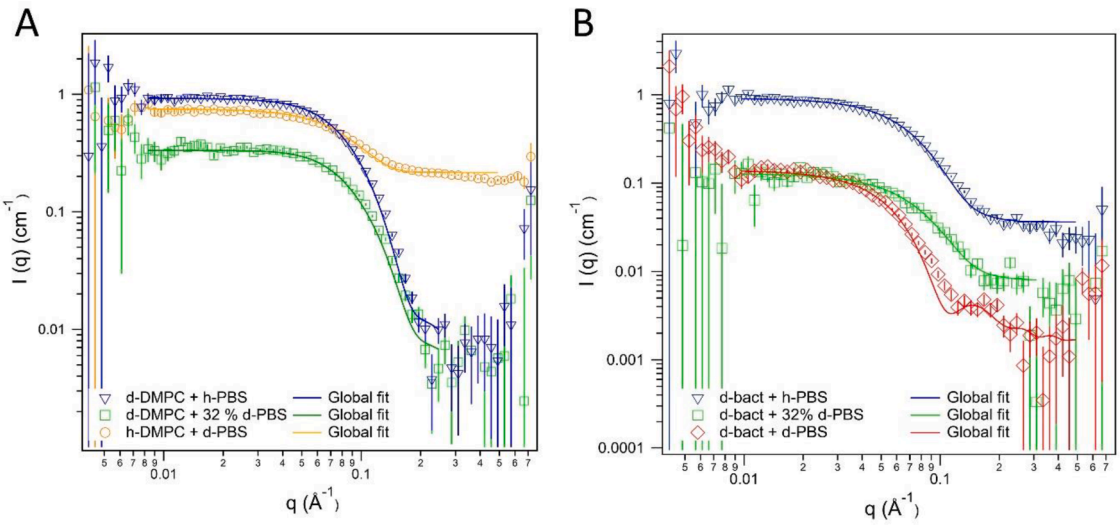

Fig. 3. [A] Individual fit of SANS data collected for gramicidin incorporated in nanodiscs using SMA2000 at three different contrast conditions. Model used; circular cylindrical nanodisc model adapted from [21]. Contrasts are as follows; ▽ deuterated DMPC (d-DMPC) with h-PBS, ○ h-DMPC with d-PBS, □ d-DMPC with 32 % d-PBS. [B] Simultaneous fit of SANS data collected for OmpF incorporated in nanodiscs using SMA2000 at three different contrast conditions. Model used; ellipsoidal cylindrical nanodisc model adapted from [44] Contrasts are as follows; ▽ partially deuterated bacterial membranes through lipid exchange with d-DMPC (d-bact) with h-PBS, ⋄ d-bact with d-PBS, □ d-bact with 32 % d-PBS. $\chi^2 = 0.032$. Data was simultaneously fitted using the NIST SANS Analysis package within the Igor Pro 6 (Wavemetrics) software [21].

OmpF-SMA sample (Peak 3, Table 2). The CD signal from DMPC-only nanodiscs was flat and was used to subtract any potential background signal and copolymer interference from the OmpF-SMA nanodisc CD spectrum. The samples from SEC P2 were also measured (data not shown). However, no signal was observed, suggesting this peak does not contain protein. Hence, the nanodiscs incorporating OmpF were only present in the Peak 3 sample from SEC.

The results shown in Table 2 indicate that the secondary structure values of OmpF-incorporated in nanodiscs vary slightly compared to the OmpF crystal structure 2OMF. This may be due to contaminants or slight impurities from the OmpF enriched sample. The values for unordered aspects are slightly higher in the OmpF-nanodisc sample, with the β-sheets value being lower as a result. This could indicate that the environment within the nanodisc is affecting the OmpF structure. SMA derived nanodiscs show negligible absorbance at these wavelengths and are well suited for investigating proteins using CD [11]. As a result, it was thought the surrounding environment was causing the conformational changes seen here, rather than direct interference from polymer absorbance. SANS data provide further insight into the structural changes observed from these CD results.

Table 3
Parameter values that are allowed to vary during fitting of the SANS data shown in Fig 3. [A] Parameter values for gramicidin-nanodiscs using the circular cylindrical nanodisc model. [B] Parameter values for OmpF-nanodiscs using the ellipsoidal cylindrical nanodisc model. [Minor radius] depicts the radius of the lipid-protein core component of the system, [radial polydispersity] depicts the polydispersity of the radius of the lipid-protein core, [Core length] depicts the length of the lipid tails / depth of the nanodisc core, [Polymer belt thickness] corresponds to the polymer belt surrounding the lipid-protein core within the nanodisc system, [Major Radius] corresponds to the second radius of the nanodisc core cross section.

A			B		
SANS Model: Circular Cylinder Nanodisc			SANS Model: Ellipsoidal Cylinder Nanodisc		
Parameters	Values	±	Parameters	Values	±
Core radius (Å)	23	1	Minor radius (Å)	15	1
radial polydispersity (σ)	0.10	0.02	Major radius (Å) (nu)	35 (2.3)	1
CORE length (Å)	28		CORE length (Å)	44	
Polymer belt thickness (Å)	8	1	Polymer belt thickness (Å)	9	1

3.4. DLS of OmpF and gramicidin samples

Prior to SANS measurements, DLS was used to measure the size of components corresponding to each of the peaks obtained from SEC. The results indicated that the nanodisc is approximately 130 Å (13 nm) in diameter in P3 (Fig. 2.D) and the corresponding polydispersity is at 0.35, prior to lipid exchange. The relatively high polydispersity may be due to the nature of the outer lipid membrane components which are expected to be heterogeneous and to include lipopolysaccharides as well as phospholipids and other components. The polydispersity may also arise from the shape of the OmpF containing nanodiscs, since the DLS analysis assumes spherical particles, whereas SANS analysis suggests that an ellipsoidal cylindrical model is a better fit to the data. The analysis discussed below demonstrates that these constructs are not spherical. The size of these nanodiscs is larger than empty DMPC-SMA nanodiscs, which are typically 80–90 Å in diameter [29], and have a low polydispersity of 0.18. DLS data obtained from P3 showed higher polydispersity than DMPC-only nanodiscs, suggesting that this sample was not purely OmpF containing nanodiscs. This polydispersity may arise from a combination of single protein species nanodiscs, empty nanodiscs and potentially the random assortment of lipids probably still associated within each nanodisc. Polydispersity tends to be much lower when observing lipid-only nanodisc samples [37,52]. After lipid-exchange using d-DMPC-containing nanodiscs, the diameter is reduced to 8.8 nm with a PDI of 0.1, similar to the DMPC-only nanodiscs. This uniformity suggests only one type of nanodisc is present, that containing OmpF, and the change in size and polydispersity suggests successful lipid-exchange from the heterogeneous native lipids from the outer membrane to largely d-DMPC lipids within the sample.

DLS data from gramicidin-nanodiscs are a similar size to lipid-only nanodiscs at approximately 80 Å (8 nm) in diameter (Fig. 2.D). This similarity in size was expected, as gramicidin monomers are small peptides of 15 amino acids [28,53], so these nanodiscs would contain mainly DMPC lipid. Therefore, the gramicidins present in the nanodiscs would not exceed the typical DMPC-nanodisc diameter and are therefore

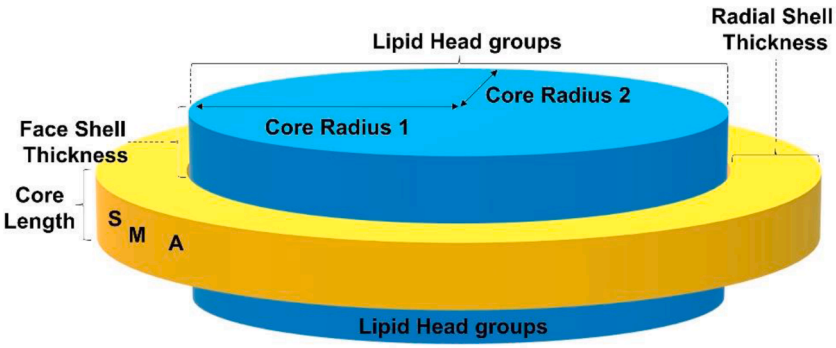

Fig. 4. SANS representative ellipsoidal cylinder nanodisc model, showing the parameters used to fit the SANS data to this model [44].

unlikely to affect the natural formation of the nanodisc with DMPC.

3.5. SANS data fitting

3.5.1. Gramicidin

Fig. 3A shows the SANS data collected from gramicidin containing nanodiscs at three different buffer contrasts. Gramicidin-nanodisc fits were generated using the circular cylindrical nanodisc model, derived from models developed at NIST [21] to incorporate water content in the shell/ polymer belt (Fig. 1). This model was deemed suitable as the peptide dimer incorporated in the nanodisc would be 30 amino acids long, and so the lipid core of the nanodisc would be largely DMPC, and this model has been used when studying lipid-only nanodiscs previously [37,54]. The gramicidin-nanodisc datasets were simultaneously fitted to obtain initial values and refined to account for the various aspects of the system highlighted in the three separate contrasts. Uncertainties in the fitted parameters were generated by repeating the fits a number of times with different starting values and noting the variation in parameter values for fits with equivalent χ^2 values. The core radius of the nanodiscs was determined to be 23 ± 1 Å, with the polymer belt being slightly thinner at 8 ± 1 Å (Table 3.A, in comparison to lipid-only nanodiscs which have a core radius typically around 10 Å [23,37,54]. The core length was fixed at 28 Å, the same value as DMPC-lipid only nanodiscs. The overall diameter of the nanodisc can be calculated as 62 Å in diameter. This is slightly smaller than the size calculated with DLS. However, the size calculated for DLS is the hydrodynamic radius calculated from the diffusion coefficient, which includes the shell of solvated counterions and solvent that move with the polymer nanodisc in the overall size.

3.5.2. OmpF

Initially, fittings were attempted using the circular cylindrical nanodisc model that had been utilised for the gramicidin-nanodiscs. However, this model did not incorporate all the aspects of the structure, and therefore gave poor fits to the data. As a result, the data for different contrasts of OmpF-incorporated in nanodiscs were simultaneously fitted using an ellipsoidal cylindrical nanodisc model (Fig. 4), which was determined to be more suitable for SANS analysis, as the fit to the data was greatly improved [44]. This model incorporates a major and minor radii aspect for the cylinder cross section. This is calculated by "nu", which depicts the ellipticity of the disc. Ellipticity is calculated as follows.

$$Major\ Radius = Minor\ Radius \cdot nu \quad (1)$$

The three contrasts were globally fitted in Igor Pro (Fig. 3B). The results indicated the cylindrical nanodisc to have an ellipsoidal rather than circular cross-section, so was an elongated flat disc, at approximately 48 Å by 88 Å in total diameter (Table 3B). The larger diameter corresponds to that measured by DLS for the lipid exchanged sample, bearing in mind that DLS assumes the particles are spherical, but also includes a hydration layer. The radial shell thickness, corresponding to the polymer bounding the edges of the lipid bilayer was calculated to be 9 ± 1 Å, similar to lipid-only nanodiscs which normally have a polymer belt around 10 Å thick [37,54,55] and to the belt on the gramicidin-nanodiscs, at approximately 8 Å. The depth of the lipid core (Table 3.B, Core length) was fixed at 44 Å; by adding the length of the lipid heads, fixed at 8 Å, the total core length will match the typical length of the OmpF at 60 Å [56]. The ellipsoidal cylinder model fitted the sample data well ($\chi^2 = 0.032$), suggesting that the nanodiscs within these samples have a more elongated core cross-section than the circular lipid only nanodiscs.

3.6. Gramicidin DAMMIN ab initio shape determination

Initially, MONSA software was applied to the multiple contrasts to perform *ab initio* shape determination. However, given the small peptide size of gramicidin (molecular weight at 1880 g/mol) it proved challenging to separate the different phases within this system. Therefore, for this system we utilised DAMMIF [47]. Only one contrast was required, d-DMPC with 32 % d-PBS, which predominantly highlights the

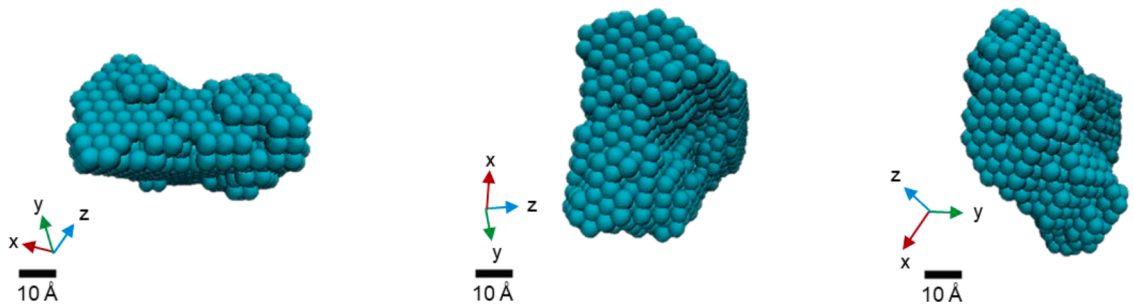

Fig. 5. DAMMIN ab initio modelling of the gramicidin SMA2000 nanodisc system [22]. This model was repeated $n = 10$. Model was run through DAMMIF, DAMSEL, DAMSUP DAMAVER and DAMFILT [45,47]. The model was visualised using Visual Molecular Dynamics (VMD) [49]. This model is shown in three different orientations. Scale bar is 10 Å. The bead colour [cyan] depicts the core of the nanodisc, including lipid, and gramicidin protein.

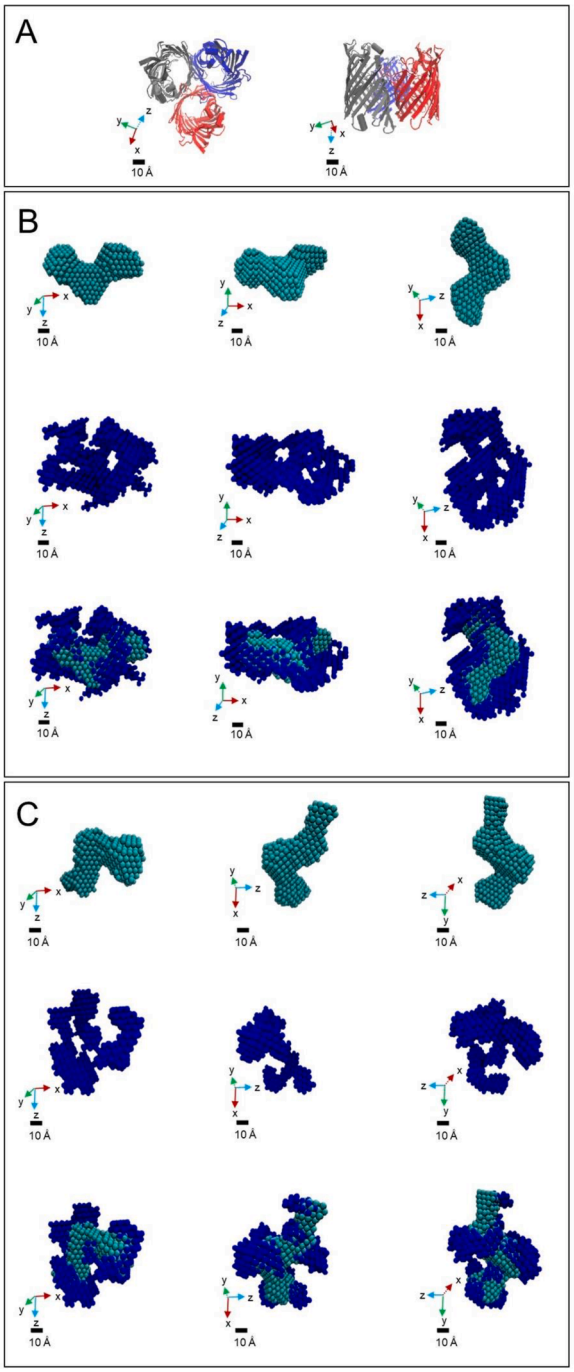

Fig. 6. MONSA *ab initio* modelling of the OmpF SMA2000 nanodisc system [22]. The model was repeated through MONSA online, $n = > 5$, with symmetry P1 (no symmetry). **[A]** shows model orientations of the crystal trimer formation of OmpF (PDB ID: 2OMF), **[B]** shows model orientations for interconnected phases, with separate contrasts, **[C]** shows model orientations for disconnected phases with separate contrasts**. [Blue]** depicts the lipid belt phase, **[Green]** shows the lipid and protein centre of the system.. **[Row 1 and 4]** represent the protein and lipid centre only, **[Row 2 and 5]** show the polymer belt component of the nanodisc, **[Row 3 and 6]** show the two phases once superimposed onto one another at the same orientation using SUPCOMB [48]. **[Columns]** depict various orientations of each model. Models were visualised using Visual Molecular Dynamics (VMD)[49]. Scale bar is 10Å.

lipid/protein core of the nanodisc, whilst masking out the polymer belt. DAMMIF was used to create an overall shape before further refinement.

After refinement, the model was passed through DAMMIN [22], to produce the finalised shape single-phase model for the gramicidin-nanodiscs, shown in three different orientations (Fig. 5). The model is approximately 70 Å across by 30 Å at the thickest point towards the edges of the disc. This size is in excellent agreement with previously derived nanodisc sizes with DMPC, around 80 Å in diameter with a core length of approximately 28 Å. Additionally, the DLS data for the gramicidin-nanodiscs show diameters around 80 Å and SANS fittings using the circular nanodisc model show an overall size of approximately 62 Å. Taking into account the variation of size for DLS, due to the hydrodynamic radius and the low-resolution models from *ab initio* refinement, these similar sizes suggest a promising route for structural analysis of the protein-incorporating nanodisc. Interestingly, as shown in Fig. 5, there is a distinct dip in the centre of the disc, approximately, 25 Å thick. This dip is consistent with insertion and dimerisation of gramicidin in the centre of the DMPC bilayer patch in the nanodisc, resulting in bilayer thinning due to hydrophobic mismatch [57]. In dimer form, gramicidin can form a channel 25 Å in length and 40 Å in diameter [53,58,59]. Here it is thought that the model illustrates both the lipid bilayer and the gramicidin dimer incorporated in the polymer nanodisc. It is uncertain at this point whether one or more dimers are present within the nanodiscs, as no difference in nanodisc size was observed when initially separated through SEC (data not shown), suggesting that only one population of nanodiscs is present, although the small size of gramicidin makes that less certain.

3.7. MONSA Parameters for Fitting OmpF Nanodisc SANS data

OmpF-nanodisc SANS samples underwent *ab initio* modelling using the MONSA web interface [22]. This software is able to simultaneously fit multi-phase datasets together into a "dummy atom" model. It is therefore indicated for use with multi-contrast SANS datasets. The model generated consists of beads or "dummy atoms" which are assigned to different phases or to the solvent. The datasets were passed through the MONSA software $n = 5$ to generate 5 separate models. Two phases were used to distinguish the OmpF protein/lipid core of the nanodisc from the polymer part of the system, based on predefined SLDs. The OmpF incorporated in the disc could be in trimer or monomer form, thus a symmetry of P3 (3 planes of symmetry) could in principle fit the SANS data – however, in this instance, it was decided due to the nature of the polymer belt surrounding the nanodiscs, that modelling with no symmetry (P1) would generate a more accurate model of the nanodisc. Therefore, this parameter was left as P1, i.e. no imposed symmetry within the system. The R_{max} was calculated at 45 Å using GNOM [60] (Appendix Fig A.2.). Three contrasts were compared using this method to attempt to distinguish between the lipid/polymer and the protein. These were d-bact with h-PBS, d-bact with d-PBS, and lastly d-bact with 32% PBS to mask out the polymer belt. Two parameters were tested using MONSA. The first was to use interconnected phases with separate contrasts which forces connectivity within each of the two phases. The second was to disconnect the phases and maintain separate contrasts.

3.8. OmpF nanodisc SANS data MONSA fittings

The MONSA models shown in Fig. 6, show two phases; the blue dummy beads correspond to the polymer belt surrounding the OmpF protein, whereas the green dummy beads correspond to the lipid/membrane protein core. Both the interconnected and disconnected phase models show a distinct elongated shape, with potentially three segments, which could in principle correspond to the trimer form of the OmpF protein. The interconnected phase model was measured at approximately 80 Å by 30 Å, whereas the disconnected phase model was slightly smaller at 70 Å by 30 Å. This coincides with the current understanding that the OmpF-nanodisc system is more ellipsoidal than

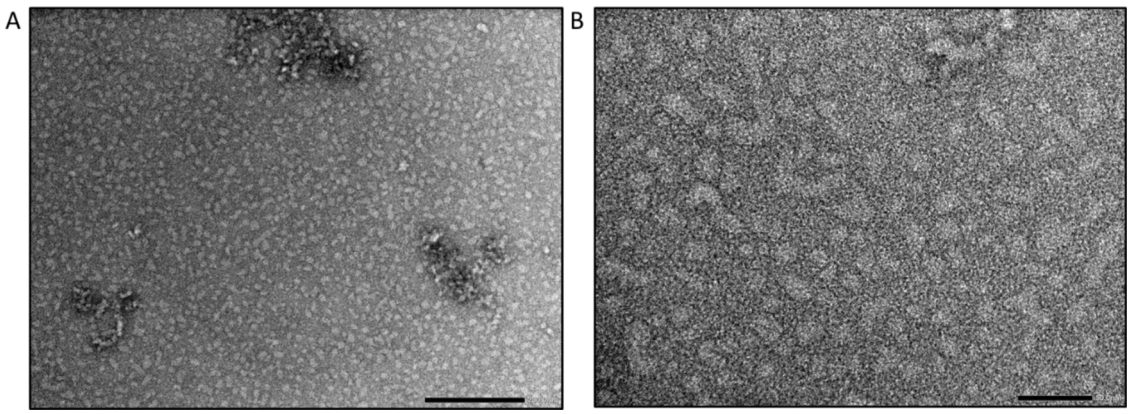

Fig. 7. TEM micrographs of OmpF bacterial membranes incorporated into polymer nanodiscs with SMA2000. [A] Scale bar represents 200 Å; [B] Scale bar represents 100 Å.

previous lipid-only and gramicidin-nanodiscs. The ellipsoidal shape could indicate that the trimer form of OmpF has been incorporated into the nanodisc, as the shape is not dissimilar to that previously found for the crystal trimer form of OmpF (PDB ID: 2OMF) (Fig. 6.A). However, it also suggests the protein has been pulled in the nanodisc into a more elongated form (Fig. 6.B and 6.C). The diameters calculated by the form factor fitted ellipsoidal nanodisc model in Fig. 3, suggested a core diameter of 30 Å by 70 Å, but with the polymer belt, the total length would be 48 Å by 88 Å. Although the shortest core diameter at 30 Å would accommodate the β-barrel, which has a diameter of 20 Å [61] at its widest point, the longest core length was considered too short to accommodate a trimer, which is approximately 100 Å in the crystal structure [33]. Although the shape of the protein aspect of the system remains similar across both parameter sets, the distribution of the blue "dummy atoms" which correspond to the polymer, does not. In the first instance, where both phases are interconnected, the polymer belt, is portrayed as a randomised chain which encircles the lipid and protein. However, with the second set of parameters that disconnect the phases, the polymer belt becomes more globular; seemingly to separate into discrete clumps around the protein/lipid core to keep it in place. With the current datasets, there is difficulty in establishing which of the two multi-phase models is most accurate. Higher level computational models and additional experimental data contrasts may help to resolve this issue. Alternatively, the extension of the protein structure could be due to the differentiation of the lipid/polymer and protein, which may be misinterpreted in the low-resolution MONSA models.

3.9. Transmission electron microscopy

To verify whether the nanodiscs incorporating OmpF were elongated, TEM was conducted to observe the overall shape of these nanodiscs. As seen in Fig. 7.B, there do appear to be at least a fraction of elongated ellipsoidal structures in the sample. The length of these structures does not exceed 1000 Å and were measured to be around 80 to 140 Å in diameter. However, further investigation with additional techniques, such as cryo-EM may be indicated.

4. Conclusion

The modelling in this study suggests that the use of *ab initio* methodologies, such as DAMMIF, DAMMIN and MONSA has the potential to aid in understanding basic aspects of the structure of proteins in polymer-nanodiscs. By comparing these models to other complimentary structure determining techniques, such as CD and DLS in this paper, these techniques combined can provide a greater understanding of the structure of both the nanodisc itself and the proteins incorporated within. The CD spectra confirmed that OmpF was incorporated into the nanodiscs. However, when compared to the published crystal structure, the OmpF-nanodisc differed considerably, suggesting the nanodisc structure could be affecting the natural folding of the protein. Conversely, due to the processes undertaken for protein crystallisation, it could be argued that the protein structure incorporated in the nanodisc could be more representative of its integral membrane form. Either would align with the results found when comparing the MONSA model. The results from DLS and SANS fitting using the form factor based nanodisc models for both gramicidin and OmpF-nanodiscs were similar when comparing the overall size. However, the *ab initio* methodologies appear to give more realistic pictures of the structure of these constructs in solution than the constrained form factor models.

The DAMMIN generated model for gramicidin-nanodiscs was shown to contain a gramicidin dimer formation at the centre of the core model, noted by a dip in the lipid/protein core. However, it was uncertain as to how many dimers may be present in the nanodiscs, as the overall size of the nanodiscs remain the same. When comparing the form factor SANS model values with those generated from MONSA fitting for OmpF-nanodiscs, we were able to determine a more elongated shape of the nanodisc, unlike lipid-only and gramicidin-nanodiscs. Although this elongation initially suggested the trimer protein may be present within the nanodiscs, we are not convinced that this is the case, as the overall length of the models were not long enough to accommodate the OmpF trimer formation. Therefore, it was suggested the OmpF trimer is either present in a non-native or differing configuration to crystal structures, or only a dimer or monomer is present within these discs. It is also thought that the idealised nanodisc shape may in reality be more complex than is generally envisaged, as the polymer phase distribution seen in both MONSA models differed from that in the deterministic form factor nanodisc model used to fit the SANS data initially. Further molecular dynamics driven approaches may be the key to determining such structures in the future.

Both the form factor model and *ab initio* model, start with the same data, however, the underlying mathematical analysis is rather different. Form factors are limited by their fixed shapes, requiring polydispersity to "blur" the structure to obtain a good fit for non-ideal or arbitrary shapes. These models are shown as defined circular or elliptical cylinders. In contrast, the *ab initio* constructs suggest the sample may not have such well-defined cylindrical components, meaning the model generates a more weblike structure for the polymer surrounding the lipid/protein core.

This study has highlighted the potential to utilise *ab initio* modelling techniques, alongside form factor analysis methods for SANS data and other structural analytical techniques, to provide an alternative structural insight when studying extracted membrane proteins in polymer nanodiscs. Further complimentary techniques help ensure that the protein in question has not been affected by incorporation into the

polymer nanodisc. In conclusion, the work here demonstrates the utility of *ab initio* modelling in determining protein structure from SANS data for proteins incorporated in polymer-nanodiscs.

Author contributions

K.A.M: Methodology, Investigation, Formal analysis, Visualization, Writing - Original Draft and Review & Editing. K.J.E: Conceptualization, Writing - Review & Editing, Supervision. J.D: Investigation of SANS data, Formal analysis, Writing - Review & Editing, Supervision. A.D: Help with Formal analysis of CD data, Writing - Review & Editing. G.N: Investigation of SANS data, Writing - Review & Editing. P.W: Writing - Review & Editing, Supervision. G.J.P: Writing - Review & Editing, Supervision.

Acknowledgements

K.A.M would like to thank the STFC (ISIS) and EPSRC for co-funding a PhD studentship via the EPSRC Centre for Doctoral Training in Sustainable Chemical Technologies (EP/L016354/1; STFC Studentship Agreement no. #SA-54). A.D is funded by the Annett Trust and the British Council Newton Fund. The authors would like to acknowledge Dr Leide Cavalcanti and Dr Marcelo Alves Da Silva for assisting with the research conducted at ISIS Neutron and Muon Source (Harwell, UK) (experiment RB1920099, DOI: 10.5286/ISIS.E.RB1920099). We would like to further acknowledge Diana Lednitzky, for the sample preparation and in obtaining the TEM images in this manuscript.

Supplementary materials

Supplementary material associated with this article can be found, in the online version, at doi:10.1016/j.bbadva.2021.100033.

References

[1] T. Ravula, S.K. Ramadugu, G. Di Mauro, A. Ramamoorthy, Bioinspired, size-tunable self-assembly of polymer–lipid bilayer nanodiscs,, Angew. Chemie - Int (2017) 11466–11470, https://doi.org/10.1002/anie.201705569.

[2] A.F. Craig, E.E. Clark, I.D. Sahu, R. Zhang, N.D. Frantz, M.S. Al-Abdul-Wahid, C. Dabney-Smith, D. Konkolewicz, G.A. Lorigan, Tuning the size of styrene-maleic acid copolymer-lipid nanoparticles (SMALPs) using RAFT polymerization for biophysical studies, Biochim. Biophys. Acta - Biomembr. 1858 (2016) 2931–2939, https://doi.org/10.1016/j.bbamem.2016.08.004.

[3] J.M. Dörr, S. Scheidelaar, M.C. Koorengevel, J.J. Dominguez, M. Schäfer, C.A. van Walree, J.A. Killian, The styrene–maleic acid copolymer: a versatile tool in membrane research, Eur. Biophys. J. 45 (2016) 3–21, https://doi.org/10.1007/s00249-015-1093-y.

[4] R.M. Bill, P.J.F. Henderson, S. Iwata, E.R.S. Kunji, H. Michel, R. Neutze, S. Newstead, B. Poolman, C.G. Tate, H. Vogel, Overcoming barriers to membrane protein structure determination, Nat. Biotechnol. 29 (2011) 335–340, https://doi.org/10.1038/nbt.1833.

[5] A.E. Rawlings, Membrane proteins: always an insoluble problem? Biochem. Soc. Trans. 44 (2016) 790–795, https://doi.org/10.1042/BST20160025.

[6] M.C. Fiori, Y. Jiang, W. Zheng, M. Anzaldua, M.J. Borgnia, G.A. Altenberg, H. Liang, Polymer nanodiscs: discoidal amphiphilic block copolymer membranes as a new platform for membrane proteins, Sci. Rep. 7 (2017) 1–9, https://doi.org/10.1038/s41598-017-15151-9.

[7] F. Bernhard, C. Klammt, H. Rüterjans, Recombinant deoxyribonucleic acid and protein expression, Compr. Med. Chem. II. (2007) 107–128, https://doi.org/10.1016/B0-08-045044-X/00079-1.

[8] D.J. Scott, L. Kummer, D. Tremmel, A. Plückthun, Stabilizing membrane proteins through protein engineering, Curr. Opin. Chem. Biol. 17 (2013) 427–435, https://doi.org/10.1016/j.cbpa.2013.04.002.

[9] M. Azouz, M. Gonin, S. Fiedler, J. Faherty, M. Decossas, C. Cullin, S. Villette, M. Lafleur, I.D. Alves, S. Lecomte, A. Ciaccafava, Microfluidic diffusional sizing probes lipid nanodiscs formation, Biochim. Biophys. Acta - Biomembr. 1862 (2020), 183215, https://doi.org/10.1016/j.bbamem.2020.183215.

[10] R. Puthenveetil, K. Nguyen, O. Vinogradova, Nanodiscs and solution NMR: preparation, application and challenges, Nanotechnol. Rev. 6 (2017) 111–125, https://doi.org/10.1515/ntrev-2016-0076.

[11] T.J. Knowles, R. Finka, C. Smith, Y.P. Lin, T. Dafforn, M. Overduin, Membrane proteins solubilized intact in lipid containing nanoparticles bounded by styrene maleic acid copolymer, J. Am. Chem. Soc. 131 (2009) 7484–7485, https://doi.org/10.1021/ja810046q.

[12] B. Danielczak, A. Meister, S. Keller, Influence of Mg2+ and Ca2+ on nanodisc formation by diisobutylene/maleic acid (DIBMA) copolymer, Chem. Phys. Lipids. 221 (2019) 30–38, https://doi.org/10.1016/j.chemphyslip.2019.03.004.

[13] S.R. Tonge, B.J. Tighe, Responsive hydrophobically associating polymers: a review of structure and properties, Adv. Drug Deliv. Rev. 53 (2001) 109–122, https://doi.org/10.1016/S0169-409X(01)00223-X.

[14] C.M. Jeffries, Z. Pietras, D.I. Svergun, The basics of small-angle neutron scattering (SANS for new users of structural biology), Eur. Phys. J. Conf. 236 (2020) 1–35, https://doi.org/https://doi.org/10.1051/epjconf/202023603001.

[15] G.I. Sackheim, An introduction to neutrons for biology, Eur. Phys. J. Conf. 236 (2008) 1–18. https://books.google.co.uk/books?id=wEWtAAAACAAJ&dq=introduction+to+chemistry&hl=en&sa=X&ved=0ahUKEwi15ryg3orbAhVKKcAKHffaBpYQ6AEIOjAD.

[16] M. Smyth, J. Martin, X-Ray Crystallography, Mol. Pathol. 53 (2000) 8–14, https://doi.org/10.1136/mp.53.1.8.

[17] E. Mahieu, F. Gabel, Biological small-angle neutron scattering: recent results and development, Acta Crystallogr. Sect. D Struct. Biol. 74 (2018) 715–726, https://doi.org/10.1107/S2059798318005016.

[18] T.M. Weiss, Small angle scattering: historical perspective and future outlook, in: B. Chaudhuri, I.G. Muñoz, V.S. Urban, S. Qian (Eds.), Biol. Small Angle Scatt. Tech. Strateg. Tips, 1009th ed.,, Eds., Springer Nature Singapore, Singapore, 2017, pp. 1–10, https://doi.org/10.1007/978-981-10-6038-0.

[19] F. Gabel, Applications of SANS to study membrane protein systems, in: B. Chaudhuri, I.G. Muñoz, V.S. Urban, S. Qian (Eds.), Biol. Small Angle Scatt. Tech. Strateg. Tips, 1009th ed., Eds., Springer Nature Singapore, Sinapore, 2017, pp. 201–214, https://doi.org/10.1007/978-981-10-6038-0.

[20] C.M. Jeffries, M.A. Graewert, C.E. Blanchet, D.B. Langley, A.E. Whitten, D. I. Svergun, Preparing monodisperse macromolecular samples for successful biological small-Angle X-ray and neutron-scattering experiments, Nat. Protoc. 11 (2016) 2122–2153, https://doi.org/10.1038/nprot.2016.113.

[21] S.R. Kline, Reduction and analysis of SANS and USANS data using IGOR Pro, J. Appl. Crystallogr. 39 (2006) 895–900, https://doi.org/10.1107/S0021889806035059.

[22] D. Svergun, Restoring low resolution structure of biological macromolecules from solution, Biophys. J. 76 (1999) 2879–2886, https://doi.org/10.1016/S0006-3495(99)77443-6.

[23] M. Jamshad, V. Grimard, I. Idini, T.J. Knowles, M.R. Dowle, N. Schofield, P. Sridhar, Y. Lin, R. Finka, M. Wheatley, O.R.T. Thomas, R.E. Palmer, M. Overduin, C. Govaerts, J.M. Ruysschaert, K.J. Edler, T.R. Dafforn, Structural analysis of a nanoparticle containing a lipid bilayer used for detergent-free extraction of membrane proteins, Nano Res 8 (2015) 774–789, https://doi.org/10.1007/s12274-014-0560-6.

[24] N. Skar-Gislinge, J.B. Simonsen, K. Mortensen, R. Feidenhans'l, S.G. Sligar, B. Lindberg Møller, T. Bjørnholm, L. Arleth, Elliptical structure of phospholipid bilayer nanodiscs encapsulated by scaffold proteins: casting the roles of the lipids and the protein, J. Am. Chem. Soc. 132 (2010) 13713–13722, https://doi.org/10.1021/ja1030613.

[25] D.G. Nicholls, S. Ferguson, Ion transport across energy- conserving membranes, in: C.E. Arnold, T.J. Chandler (Eds.), Bioenerg. 3, 3rd ed., Eds., Academic Press, New York, 2002, pp. 17–28.

[26] D.G. Nagle, Y.D. Zhou, Natural products as probes of selected targets in tumor cell biology and hypoxic signaling. Compr. Nat. Prod. II Chem. Biol., Elsevier Ltd., 2010, pp. 651–683, https://doi.org/10.1016/b978-008045382-8.00054-x.

[27] J.A. Doebler, Effects of neutral ionophores on membrane electrical characteristics of NG108-15 cells, Toxicol. Lett. 114 (2000) 27–38, https://doi.org/10.1016/S0378-4274(99)00193-9.

[28] J.M. David, A.K. Rajasekaran, Gramicidin A: a new mission for an old antibiotic, J. Kidney Cancer VHL. 2 (2015) 15–24, https://doi.org/10.15586/jkcvhl.2015.21.

[29] M.C. Orwick, P.J. Judge, J. Procek, L. Lindholm, A. Graziadei, A. Engel, G. Gröbner, A. Watts, Detergent-free formation and physicochemical characterization of nanosized lipid-polymer complexes: Lipodisq, Angew. Chemie - Int. Ed 51 (2012) 4653–4657, https://doi.org/10.1002/anie.201201355.

[30] S.W. Cowan, R.M. Garavito, J.N. Jansonius, J.A. Jenkins, R. Karlsson, N. König, E. F. Pai, R.A. Pauptit, P.J. Rizkallah, J.P. Rosenbusch, G. Rummel, T. Schirmer, The structure of OmpF porin in a tetragonal crystal form, Structure 3 (1995) 1041–1050, https://doi.org/10.1016/S0969-2126(01)00240-4.

[31] A. Engel, Atomic force Microscopy and Electron Microscopy of Membrane Proteins, Elsevier Ltd., 2012, https://doi.org/10.1016/B978-0-12-374920-8.00511-7.

[32] J.P. Rosenbusch, Characterization of the major envelope protein from Escherichia coli. Regular arrangement on the peptidoglycan and unusual dodecyl sulfate binding, J. Biol. Chem. 249 (1974) 8019–8029, https://doi.org/10.1016/S0021-9258(19)42066-8.

[33] G. Kefala, C. Ahn, M. Krupa, L. Esquivies, I. Maslennikov, W. Kwiatkowski, S. Choe, Structures of the OmpF porin crystallized in the presence of foscholine-12, Protein Sci 19 (2010) 1117–1125, https://doi.org/10.1002/pro.369.

[34] X. Wang, D. Teng, Q. Guan, R. Mao, Y. Hao, X. Wang, J. Yao, J. Wang, Escherichia coli outer membrane protein F (OmpF): an immunogenic protein induces cross-reactive antibodies against Escherichia coli and Shigella, AMB Express 7 (2017) 1–12, https://doi.org/10.1186/s13568-017-0452-8.

[35] K.M. Williams, E.C. Bigley, R.B. Raybourne, Identification of murine B-cell and T-cell epitopes of Escherichia coli outer membrane protein F with synthetic polypeptides, Infect. Immun. 68 (2000) 2535–2545, https://doi.org/10.1128/IAI.68.5.2535-2545.2000.

[36] S.W. Cowan, T. Schirmer, G. Rummel, M. Steiert, R. Ghosh, R.A. Pauptit, J. N. Jansonius, J.P. Rosenbusch, Crystal structures explain functional properties of

two E. coli porins, Nature 358 (1992) 727–733, https://doi.org/10.1038/358727a0.
[37] S.C.L. Hall, C. Tognoloni, G.J. Price, B. Klumperman, K.J. Edler, T.R. Dafforn, T. Arnold, Influence of Poly(styrene- co -maleic acid) Copolymer Structure on the Properties and Self-Assembly of SMALP Nanodiscs, Biomacromolecules 19 (2018) 761–772, https://doi.org/10.1021/acs.biomac.7b01539.
[38] S.C.L. Hall, L.A. Clifton, C. Tognoloni, K.A. Morrison, T.J. Knowles, C.J. Kinane, T. R. Dafforn, K.J. Edler, T. Arnold, Adsorption of a styrene maleic acid (SMA) copolymer-stabilized phospholipid nanodisc on a solid-supported planar lipid bilayer, J. Colloid Interface Sci. 574 (2020) 272–284, https://doi.org/10.1016/j.jcis.2020.04.013.
[39] R.G. Efremov, L.A. Sazanov, Structure of Escherichia coli OmpF porin from lipidic mesophase, J. Struct. Biol. 178 (2012) 311–318, https://doi.org/10.1016/j.jsb.2012.03.005.
[40] A. Lobley, L. Whitmore, B.A. Wallace, DICHROWEB: an interactive website for the analysis of protein secondary structure from circular dichroism spectra, Bioinformatics 18 (2002) 211–212, https://doi.org/10.1093/bioinformatics/18.1.211.
[41] L. Whitmore, B.A. Wallace, Protein secondary structure analyses from circular dichroism spectroscopy: Methods and reference databases, Biopolymers 89 (2008) 392–400, https://doi.org/10.1002/bip.20853.
[42] L. Whitmore, B.A. Wallace, DICHROWEB, an online server for protein secondary structure analyses from circular dichroism spectroscopic data, Nucleic Acids Res 32 (2004) 668–673, https://doi.org/10.1093/nar/gkh371.
[43] O. Arnold, J.C. Bilheux, J.M. Borreguero, A. Buts, S.I. Campbell, L. Chapon, M. Doucet, N. Draper, R. Ferraz Leal, M.A. Gigg, V.E. Lynch, A. Markvardsen, D. J. Mikkelson, R.L. Mikkelson, R. Miller, K. Palmen, P. Parker, G. Passos, T. G. Perring, P.F. Peterson, S. Ren, M.A. Reuter, A.T. Savici, J.W. Taylor, R.J. Taylor, R. Tolchenov, W. Zhou, J. Zikovsky, Mantid - Data analysis and visualization package for neutron scattering and μ SR experiments, Nucl. Instruments Methods Phys. Res. Sect. A Accel. Spectrometers, Detect. Assoc. Equip 764 (2014) 156–166, https://doi.org/10.1016/j.nima.2014.07.029.
[44] D. Singh, Small Angle Scattering Studies of Self Assembly in Lipid Mixtures, The Johns Hopkins University, Baltimore, Maryland, 2008. PhD Thesis.
[45] V.V. Volkov, D.I. Svergun, Uniqueness of ab initio shape determination in small-angle scattering, J. Appl. Crystallogr. 36 (2003) 860–864, https://doi.org/10.1107/S0021889803000268.
[46] J. Trewhella, A.P. Duff, D. Durand, F. Gabel, J.M. Guss, W.A. Hendrickson, G. L. Hura, D.A. Jacques, N.M. Kirby, A.H. Kwan, J. Pérez, L. Pollack, T.M. Ryan, A. Sali, D. Schneidman-Duhovny, T. Schwede, D.I. Svergun, M. Sugiyama, J. A. Tainer, P. Vachette, J. Westbrook, A.E. Whitten, 2017 publication guidelines for structural modelling of small-angle scattering data from biomolecules in solution: an update, Acta Crystallogr. Sect. D. 73 (2017) 710–728, https://doi.org/10.1107/S2059798317011597.
[47] D. Franke, D.I. Svergun, DAMMIF, a program for rapid ab-initio shape determination in small-angle scattering, J. Appl. Crystallogr. 42 (2009) 342–346, https://doi.org/10.1107/S0021889809000338.
[48] M.B. Kozin, D.I. Svergun, Automated matching of high- and low-resolution structural models, J. Appl. Crystallogr. 34 (2001) 33–41, https://doi.org/10.1107/S0021889800014126.
[49] W. Humphrey, A. Dalke, K. Schulten, {VMD} – {V}isual {M}olecular {D}ynamics, J. Mol. Graph. 14 (1996) 33–38.
[50] E.D. Drew, R.W. Janes, PDBMD2CD: providing predicted protein circular dichroism spectra from multiple molecular dynamics-generated protein structures, Nucleic Acids Res 48 (2020) W17–W24, https://doi.org/10.1093/nar/gkaa296.
[51] D. Frishman, P. Argos, Knowledge-based protein secondary structure assignment, Proteins Struct. Funct. Genet. 23 (1995) 566–579, https://doi.org/10.1002/prot.340230412.
[52] M.C. Fiori, W. Zheng, E. Kamilar, G. Simiyu, G.A. Altenberg, H. Liang, Extraction and reconstitution of membrane proteins into lipid nanodiscs encased by zwitterionic styrene-maleic amide copolymers, Sci. Rep. 10 (2020) 9940, https://doi.org/10.1038/s41598-020-66852-7.
[53] F. Wang, L. Qin, C.J. Pace, P. Wong, R. Malonis, J. Gao, Solubilized gramicidin A as potential systemic antibiotics, ChemBioChem 13 (2012) 51–55, https://doi.org/10.1002/cbic.201100671.
[54] S.C.L. Hall, C. Tognoloni, J. Charlton, É.C. Bragginton, A.J. Rothnie, P. Sridhar, M. Wheatley, T.J. Knowles, T. Arnold, K.J. Edler, T.R. Dafforn, An acid-compatible co-polymer for the solubilization of membranes and proteins into lipid bilayer-containing nanoparticles, Nanoscale 10 (2018) 10609–10619, https://doi.org/10.1039/c8nr01322e.
[55] S.C. Lee, S. Khalid, N.L. Pollock, T.J. Knowles, K. Edler, A.J. Rothnie, O. R.T. Thomas, T.R. Dafforn, Encapsulated membrane proteins: a simplified system for molecular simulation, Biochim. Biophys. Acta - Biomembr. 1858 (2016) 2549–2557, https://doi.org/10.1016/j.bbamem.2016.02.039.
[56] W. Arunmanee, J.R. Harris, J.H. Lakey, Outer membrane protein f stabilised with minimal amphipol forms linear arrays and LPS-dependent 2D Crystals, J. Membr. Biol. 247 (2014) 949–956, https://doi.org/10.1007/s00232-014-9640-5.
[57] M. Goulian, O.N. Mesquita, D.K. Fygenson, C. Nielsen, O.S. Andersen, A. Libchaber, Gramicidin channel kinetics under tension, Biophys. J. 74 (1998) 328–337, https://doi.org/10.1016/S0006-3495(98)77790-2.
[58] G.R. Marshall, D.D. Beusen, G.V Nikiforovich, Peptide conformation: stability and dynamics, in: G. Bernd (Ed.), Peptides, Academic Press, Ed., London, San Diego, 1995, pp. 193–245, https://doi.org/10.1016/B978-0-12-310920-0.50006-1.
[59] P.L. Yeagle, Membrane transport. Membr. Cells, 2nd ed., Academic Press, San Diego; London, 2016, pp. 335–378, https://doi.org/10.1016/b978-0-12-800047-2.00013-9.
[60] D.I. Svergun, Determination of the regularization parameter in indirect-transform methods using perceptual criteria, J. Appl. Crystallogr. 25 (1992) 495–503, https://doi.org/10.1107/S0021889892001663.
[61] N. Saint, K.L. Lou, C. Widmer, M. Luckey, T. Schirmer, J.P. Rosenbusch, Structural and functional characterization of OmpF porin mutants selected for larger pore size. II. Functional characterization, J. Biol. Chem. 271 (1996) 20676–20680, https://doi.org/10.1074/jbc.271.34.20676.